Constraining the low-energy pion electromagnetic form factor with spacelike data

B. Ananthanarayan[a], S. Ramanan[b]

Centre for High Energy Physics, Indian Institute of Science, Bangalore 560 012, India

Abstract. The pionic contribution to the $g-2$ of the muon involves a certain integral over the modulus squared of $F_\pi(t)$, the electromagnetic form factor of the pion. We extend techniques that use cut-plane analyticity properties of $F_\pi(t)$ in order to account for present day estimates of the pionic contribution and experimental information at a finite number of points in the spacelike region. Using data from several experiments over a large kinematic range for $|t|$, we find bounds on the expansion coefficients of $F_\pi(t)$, sub-leading to the charge radius. The value of one of these coefficients in chiral perturbation theory respects these bounds. Furthermore, we present a sensitivity analysis to the inputs. A brief comparison with results in the literature that use observables other than the $g-2$ and timelike data is presented.

1 Introduction

General principles such as analyticity and unitarity have been used to derive useful constraints on the form factors (for a review see [1]). In particular, useful lower bounds were obtained on the pionic contribution to the $(g-2)$ of the muon (muon anomaly). For recent reviews on the current status of this quantity, see [2, 3]. Consider the following low-energy expansion for the pion electromagnetic form factor $F_\pi(t)$:

$$F_\pi(t) = F_\pi(0) + \frac{r_\pi^2}{6}t + ct^2 + dt^3 + \cdots, \qquad (1)$$

where r_π is the pion charge radius, c and d are Taylor coefficients, with units of GeV^{-4} and GeV^{-6}, respectively. For a recent discussion, refer [7]. From general principles, discussed in the next section, and using the normalization $F_\pi(0) = 1$, one immediately finds a lower bound of $\approx 1.6 \times 10^{-9}$. Imposing the experimental value of r_π further improves the bound to 2.9×10^{-9} [4]. Caprini [5] has more recently shown that if one were to assume that the pionic contribution is less than $I = 75 \times 10^{-9}$, then these principles yield constraints on the higher expansion coefficients, c and d, which translate into an allowed ellipse in the c–d plane. These results, as well as the results we present here, hold as long as the true pionic contribution is less than the value of I we have assumed. If the pionic contribution is indeed significantly smaller, then the true allowed region would be a proper subset of the region we isolate.

The inclusion of experimental data from the timelike region, the phase, the modulus, and the phase as well as the modulus each improves the bound on the muon anomaly [1]. Using I as input, Caprini has used dispersive techniques and timelike data and has considered other physical observables such as certain QCD polarization functions, in addition to the muon anomaly, to constrain further the allowed regions in the c–d plane[1]. We note that the parameter c itself has been determined to 2-loop accuracy in chiral perturbation theory [7], and it has a value of $4.49\,\mathrm{GeV}^{-4}$, which is safely accommodated in the allowed ellipse of Caprini [5].

An important source of experimental information is the values of the electromagnetic form factor in the spacelike region. These have been reported in electroproduction experiments conducted in the 1970's [8–10]. Raina and Singh [11] used this information to produce improved bounds on the muon anomaly [12]. New experimental data are now available [13–16]. In this work, we will make use of some of the data sets above.

Our main purpose in this work is to demonstrate that the framework of Raina and Singh can effectively be used to obtain constraints in the c–d plane, using the pionic contribution to the muon anomaly as input. This is an algebraic framework, which is clear cut and transparent. It provides an important consistency check on the allowed regions isolated by Caprini.

In Sect. 2 we briefly review the dispersive formalism and describe the implementation of spacelike constraints and the method by which we isolate the region in the c–d plane. Here, we provide the theoretical framework and also a discussion on the present experimental status, as they

---

[a] e-mail: anant@cts.iisc.ernet.in
[b] e-mail: suna@cts.iisc.ernet.in

[1] Applications to form factors in semi-leptonic decays of such general methods in a modern context have also recently been considered [6].

are both required for this purpose. In Sect. 3 we present our results using data from [8–10] and more recent data from [15, 16]. We present a detailed discussion of our results and our conclusions in Sect. 4.

2 Formalism

We recall the formalism presented in [11]. The pion contribution to the muon anomaly is given by

$$a_\mu(\pi^+\pi^-) = \frac{1}{\pi}\int_{t_\pi}^\infty \mathrm{d}t\rho(t)|F_\pi(t)|^2\,, \qquad (2)$$

where $t_\pi = 4m_\pi^2$ is the branch point of the pion form factor and

$$\rho(t) = \frac{\alpha^2 m_\mu^2}{12\pi}\frac{(t-t_\pi)^{3/2}}{t^{7/2}}K(t) \ge 0\,, \qquad (3)$$

where

$$K(t) = \int_0^1 \mathrm{d}u(1-u)u^2\left(1-u+\frac{m_\mu^2 u^2}{t}\right)^{-1}\,. \qquad (4)$$

Using the following map from the t-plane, which is cut from t_π along the real t axis, to the complex z-plane (region $|z|<1$):

$$\frac{z-1}{z+1} = \mathrm{i}\sqrt{\frac{t-t_\pi}{t_\pi}} \qquad (5)$$

and the definitions

$$f(z) = F_\pi(t)\,, \qquad (6)$$
$$p(z) = \rho(t)\,, \qquad (7)$$

the pionic contribution to the muon anomaly can be written

$$a_\mu\left(\pi^+\pi^-\right) = \frac{1}{2\pi}\int_0^{2\pi}\mathrm{d}\theta w(\theta)\left|f\left(\mathrm{e}^{\mathrm{i}\theta}\right)\right|^2\,, \qquad (8)$$

where

$$w(\theta) = 4m_\pi^2\sec^2(\theta/2)\tan(\theta/2)\,p\left(\mathrm{e}^{\mathrm{i}\theta}\right) \ge 0\,. \qquad (9)$$

We now consider a function $h(z)$ defined by

$$h(z) = f(z)w_\pi(z)\,, \qquad (10)$$

where

$$w_\pi(z) = \exp\left[\frac{1}{4\pi}\int_0^{2\pi}\mathrm{d}\theta\frac{\mathrm{e}^{\mathrm{i}\theta}+z}{\mathrm{e}^{\mathrm{i}\theta}-z}\ln w(\theta)\right]\,. \qquad (11)$$

Then (8) can be written

$$a_\mu(\pi^+\pi^-) = \frac{1}{2\pi}\int_0^{2\pi}\mathrm{d}\theta\left|h\left(\mathrm{e}^{\mathrm{i}\theta}\right)\right|^2\,. \qquad (12)$$

Now $h(z)$ is analytic within the unit circle $|z|<1$, and for real z, $h(z)$ is real. Therefore $h(z)$ can be expanded as follows:

$$h(z) = a_0 + a_1 z + a_2 z^2 + \cdots\,, \qquad (13)$$

where $a_0, a_1\cdots$ are real coefficients. Therefore, in the analytic region, $|z|\le 1$, $a_\mu(\pi^+\pi^-)$ can be written as

$$a_\mu(\pi^+\pi^-) = a_0^2 + a_1^2 + \cdots\,. \qquad (14)$$

The expansion coefficients a_n can be obtained from a Taylor expansion of the function $h(z)$ in terms of $f(z)$ and $w_\pi(z)$. The coefficients are given by

$$a_0 = h(0) = w_\pi(0)\,, \qquad (15)$$

$$a_1 = h'(0) = w_\pi'(0) + \frac{2}{3}r_\pi^2 t_\pi w_\pi(0)\,, \qquad (16)$$

$$a_2 = \frac{h''(0)}{2!} = \frac{1}{2}\left[w_\pi(0)\left(-\frac{8}{3}r_\pi^2 t_\pi + 32ct_\pi^2\right)\right]$$
$$+ \frac{1}{2}\left[2w_\pi'(0)\left(\frac{2}{3}r_\pi^2 t_\pi\right) + w_\pi''(0)\right] \qquad (17)$$

and

$$a_3 = \frac{h'''(0)}{3!} = \frac{1}{6}\left[w_\pi(0)\left(12r_\pi^2 t_\pi - 384ct_\pi^2 + 384dt_\pi^3\right)\right]$$
$$+ \frac{1}{6}\left[3w_\pi'(0)\left(-\frac{8}{3}r_\pi^2 t_\pi + 32ct_\pi^2\right)\right]$$
$$+ \frac{1}{6}\left[2w_\pi''(0)r_\pi^2 t_\pi + w_\pi'''(0)\right]\,. \qquad (18)$$

In our treatment, the expansion coefficients satisfy

$$\sum_{i=0}^\infty a_i^2 = I\,. \qquad (19)$$

Given I, (19) yields constraints on the expansion coefficients of the form factor. Including up to the second (third) derivative for $F_\pi(t)$ results in constraints for c (c and d). It may be pointed out that Caprini's result on c and d shown in Fig. 1 (dashed lines) of [5] is obtained precisely in this manner.

The constraints on the expansion coefficients of interest may be significantly improved through the inclusion of experimental information on the form factor. Our objective in this work is to study the effect of including experimental information coming from the spacelike region. In order to meet this objective, we first extend the formalism that has been presented in [11]. In that work, spacelike constraints were used to obtain lower bounds on the muon anomaly, denoted as $I_{\min}$.

We observe that N spacelike constraints are linear constraints that may be expressed as

$$A_n = \sum_{i=0}^\infty a_i c_i^{(n)}\,, \qquad (20)$$

where $n = 1, 2, \cdots N$. Such constraints can be implemented through the technique of Lagrange multipliers, by setting

up the Lagrangian

$$L = \frac{1}{2}\sum_{i=0}^{\infty}a_i^2 + \sum_{n=1}^{N}\alpha_n\left(A_n - \sum_{i=0}^{\infty}a_ic_i^{(n)}\right), \qquad (21)$$

where in (21), we consider only a finite number of expansion coefficients. The Lagrange equations yield

$$a_i = \sum_{n=1}^{N}\alpha_n c_i^{(n)} \qquad (22)$$

and

$$I = \sum_{n=1}^{N}\alpha_n\sum_{i=0}^{\infty}a_ic_i^{(n)}. \qquad (23)$$

It then follows that

$$I_{\min} = \sum_{n=1}^{N}\alpha_n A_n, \qquad (24)$$

where

$$A_n = \sum_{m=1}^{N}\alpha_m\sum_{i=0}^{\infty}c_i^{(m)}c_i^{(n)}. \qquad (25)$$

All the α_n may be eliminated to yield a determinantal equation for I:

$$\begin{vmatrix} I & A_1 & A_2 & ... \\ A_1 & \sum c_i^{(1)}c_i^{(1)} & \sum c_i^{(1)}c_i^{(2)} & ... \\ A_2 & \sum c_i^{(2)}c_i^{(1)} & \sum c_i^{(2)}c_i^{(2)} & ... \\ . & ... & ... & ... \\ . & ... & ... & ... \\ . & ... & ... & ... \end{vmatrix} = 0. \qquad (26)$$

For the case at hand, where we wish to specify a_0, a_1, a_2, a_3 and the value at spacelike points $h(x_i)$, $i = 1, 2, 3, ...$, where x_i is real, the determinantal equation reads

$$\begin{vmatrix} I & a_0 & a_1 & a_2 & a_3 & h(x_1) & h(x_2) & ... \\ a_0 & 1 & 0 & 0 & 0 & 1 & 1 & ... \\ a_1 & 0 & 1 & 0 & 0 & x_1 & x_2 & ... \\ a_2 & 0 & 0 & 1 & 0 & x_1^2 & x_2^2 & ... \\ a_3 & 0 & 0 & 0 & 1 & x_1^3 & x_2^3 & ... \\ h(x_1) & 1 & x_1 & x_1^2 & x_1^3 & (1-x_1^2)^{-1} & (1-x_1x_2)^{-1} & ... \\ h(x_2) & 1 & x_2 & x_2^2 & x_2^3 & (1-x_2x_1)^{-1} & (1-x_2^2)^{-1} & ... \\ . & ... & ... & ... & ... & ... & ... \\ . & ... & ... & ... & ... & ... & ... \\ . & ... & ... & ... & ... & ... & ... \end{vmatrix}$$
$$= 0. \qquad (27)$$

In the above merely retaining the first two rows and columns gives the first bound of Palmer, given in the introduction, while retaining the first three rows and columns yields the second of Palmer's bounds. Raina and Singh [11] use the value of $F_\pi(0) = 1$ and r_π to obtain the lower bound to $a_\mu(\pi^+\pi^-)$. This amounts to dropping the rows

and columns corresponding to a_2 and a_3 in (27), which are related to the expansion coefficients c and d. Instead, providing an input to I in (27) gives us an allowed region in the c–d plane. Dropping the row and column corresponding to a_3 would result in determining an allowed region for c alone, which we pursue in the next section for purposes of illustration.

In the next subsection, we provide a discussion on the present day experimental information that is utilized in our study. This information spans an impressive range of energies, viz. $|t|$. While in principle there is no limit to the number of constraints, in practice the uncertainties in the experimental determination and sensitivity of the determinantal equation limits this number. The reason for such restrictions is the extreme sensitivity of the matrices to these experimental uncertainties as their dimensions increase. This sensitivity is particularly severe for small values of $|t|$. As a result, at such values we are able to implement at most two constraints, while data from higher energies allow us to implement up to three constraints. However, the data from smaller values of $|t|$ provide more stringent bounds for a fixed number of constraints. Thus we see a fairly complex interplay between the energy regime that we can use and the number of constraints we are able to implement.

2.1 Spacelike data

We will begin with the data in the spacelike region that was used in the work of Raina and Singh [11], that came from measurements in the seventies. We shall refer to these as the Brown data and Bebek data, respectively. The data we use from these sets are given in Tables 1 and 2. The tables also list the values of $z(t) = x(t)$, which is the map from the t-plane to the disc $|z| \leq 1$ ($x(t)$ lies in the range $[-1 \leq x(t) \leq 0]$), for the chosen data points and the corresponding value of $h(z) = h(x)$ (refer to (10)). To make our notation clear, we refer to the data points corresponding to a particular $|t|$ as x_1, x_2 and so on, in the ascending order of magnitude of $|t|$. The tables also show the experimental errors in the data.

More recent data come from four sources. The first of these are in [13], which are from a Fermilab experiment

Table 1. Spacelike data from Bebek et al. [10]

	$t(-Q^2)$ [GeV^2]	$F_\pi(t)$	$x(t)$	$h(x) \times 10^{-5}$
1	-0.620	0.453 ± 0.014	-0.499	3.057
2	-1.216	0.292 ± 0.026	-0.606	2.035
3	-1.712	0.246 ± 0.017	-0.655	1.716

Table 2. Spacelike data from Brown et al. [9]

	$t(-Q^2)$ [GeV^2]	$F_\pi(t)$	$x(t)$	$h(x) \times 10^{-5}$
1	-0.294	0.606 ± 0.028	-0.372	3.775
2	-0.795	0.380 ± 0.013	-0.540	2.608

Table 3. Spacelike data from Tadevosyan et al. [16]

	$t(-Q^2)$ [GeV^2]	$F_\pi(t)$	$x(t)$	$h(x) \times 10^{-5}$
1	-0.600	0.433 ± 0.017	-0.494	2.915
2	-1.000	0.312 ± 0.016	-0.576	2.163
3	-1.600	0.233 ± 0.014	-0.645	1.626

Table 4. Spacelike data from Amendolia et al. [15]

	$t(-Q^2)$ [GeV^2]	$F_\pi(t)$	$x(t)$	$h(x) \times 10^{-5}$
1	-0.131	0.807 ± 0.015	-0.242	4.454
2	-0.163	0.750 ± 0.016	-0.275	4.286

(F1). Here the range is $0.03\,\mathrm{GeV}^2 \leq -t \leq 0.07\,\mathrm{GeV}^2$. Even at the high end, we are way below the lowest energy of Brown. The next set of data come from another Fermi lab experiment (F2) [14], covering the range of $0.037\,\mathrm{GeV}^2 \leq -t \leq 0.094\,\mathrm{GeV}^2$. The CERN NA7 experiment provides very accurate data [15] in the range $0.014\,\mathrm{GeV}^2 \leq -t \leq 0.26\,\mathrm{GeV}^2$ (by Amendolia et al.). There is an overlap region between this last set and the Brown data and the two are consistent. The final data we use come from the JLab experiments (Tadevosyan et al. [16]).

In our study we choose to work with recent data from Amendolia et al. [15], which cover both the low and intermediate energy range (note that the data from [13, 14] cover a smaller energy range; hence our choice) and the data from the JLab experiments (Tadevosyan et al. [16]), which cover a higher range of $|t|$. Using really small $|t|$ values leads to numerical instabilities as the entries in the determinant (27) become small.

Tables 1–4 show the data that are used in our analysis to constrain the expansion coefficients c and d of the form factor $F_\pi(t)$. The data from various experiments are chosen so as to give reliable numerical results. We find the data in the lower $|t|$ to constrain the expansion coefficients better but we cannot include more than two spacelike constraints; while the higher $|t|$ region gives a weaker bound, which can be improved by increasing the number of spacelike constraints.

3 Results

In our results, we use $I = 75 \times 10^{-9}$ as input [5]. This value is certainly greater than a recent estimate for the hadronic contribution to $a_\mu^{\mathrm{had}} = 69.2 \times 10^{-9}$ [3]. The pionic contribution is expected to be around 70% of the total hadronic value. Our value for I gives a conservative upper bound to the pionic contribution to a_μ.

We begin by constraining only the expansion coefficient c, which amounts to dropping out the row and column corresponding to a_3 in (27). We determine the bounds on c in stages, starting with only the pion charge radius r_π and the normalization of $F_\pi(t)$ at $t = 0$ (i.e., no spacelike constraints) and then incorporate spacelike constraints succes-
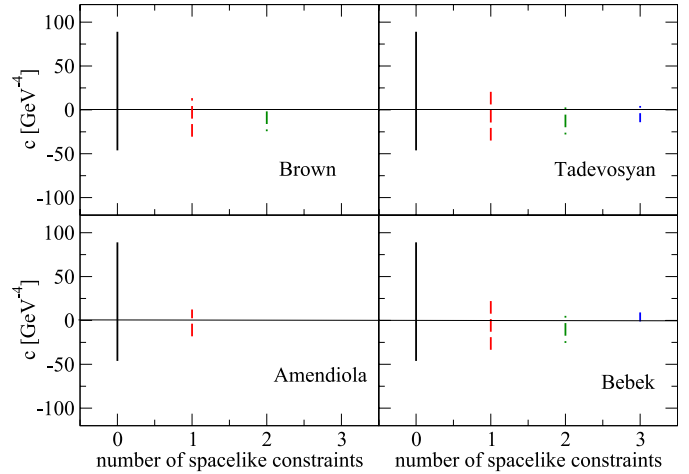

Fig. 1. Constraints on c starting with just information on $F_\pi(0) = 1$ and r_π^2 and incorporating spacelike constraints. Notice that the allowed values of c decrease as we include more spacelike constraints

sively. The results are shown in Fig. 1, where we have used data from Tables 1–4. For any data set, we start with the smallest value of $|t|$ for one spacelike constraint and include more constraints in increasing magnitude of $|t|$. All the data sets show the trend that inclusion of more spacelike constraints in this manner improves the bounds on c. The largest range for c in units of GeV^{-4} is obtained when no spacelike constraints are used. This agrees with the result of Caprini (Fig. 1 in [5]). Note, however, that for data from larger values of $|t|$, the bound on c is significantly weaker compared to data from smaller values of $|t|$ for a fixed number of spacelike constraints.

It is worth investigating the sensitivity of the bounds to the errors in the data. The Brown data shift the bounds on c to negative values when two spacelike constraints are used. This shift is sensitive to the error bounds on $F_\pi(t)$. If we use as input $F_\pi(t_1) + 0.028$ (Table 2) for the first constraint and $F_\pi(t_2) - 0.013$ for the second constraint, then
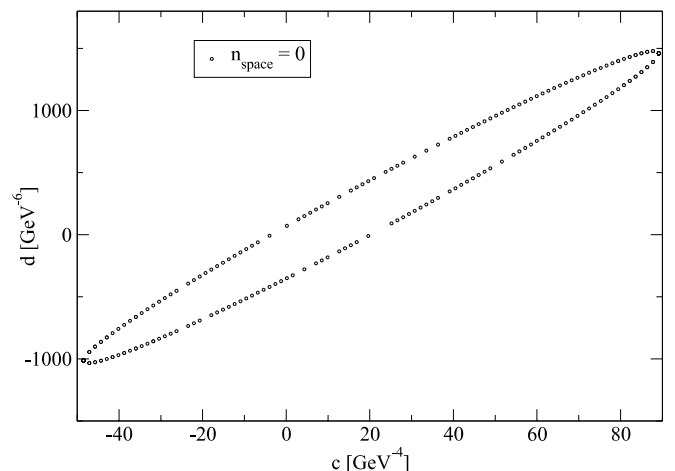

Fig. 2. Constraints on c and d using the normalization $F_\pi(0) = 1$ and the pion charge radius r_π

the upper bound on c is positive. Here, t_1 and t_2 represent the first and second data point respectively in Table 2. We present a further sensitivity analysis later in this section. Similarly for the data from Amendolia et al. [15], we see that one spacelike constraint can be incorporated using central values for $F_\pi(t)$; but varying this input over the error bounds given in Table 4, we can use up to two constraints (not shown here). Unless otherwise specified, all results presented in this section use the central values of the form factor data given in Tables 1–4.

Including constraints from a_3 results in a relationship between the expansion coefficients c and d, which we shall now explore. Figure 2 shows the allowed region in the c–d plane using only the normalization condition on $F_\pi(t)$ and the value of r_π. Analogous to the study of the bounds on c, we can include spacelike constraints to impose stringent

bounds on the expansion coefficients c and d, that are reflected by smaller allowed regions in the c–d plane. Figure 3 shows the variation in the bounds on c and d for one spacelike constraint, where data from a different $|t|$ region are used. In the figure, $h(x_1)$ is the value of $h(x)$ as defined in (10), corresponding to the smallest value of t in each data set (refer to Tables 1–4). Similarly $h(x_2)$ is the constraint at a higher $|t|$ value, taken in the ascending order of magnitude. It may readily be observed that the most stringent bounds are obtained when data from the smallest values of $|t|$ are used, and they improve as the number of constraints are increased, as noted earlier.

Figure 4 (as well as 5) shows that increasing the number of spacelike constraints improves the bounds on the expansion coefficients c and d. We observe that the allowed range for c corresponds to that in Fig. 1. Using the cen-
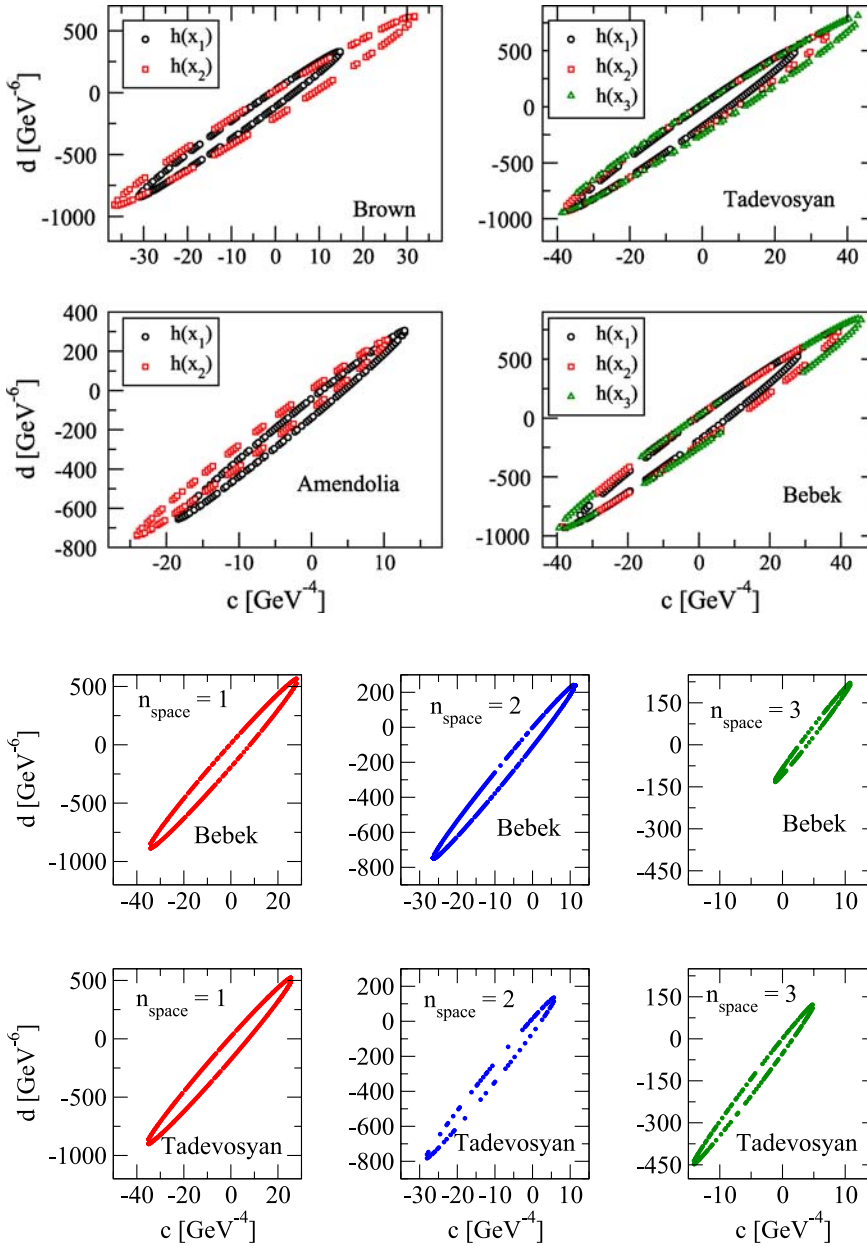

Fig. 3. Constraints on c and d using one spacelike constraint. Here we start with the smallest $|t|$ value and the corresponding value of $h(z) = h(x_1)$ and study the variation of the bounds on c and d as we use data from the higher $|t|$ region

Fig. 4. Constraints on c and d as the number of spacelike constraints are increased. Here the spacelike data are taken from [10, 16]
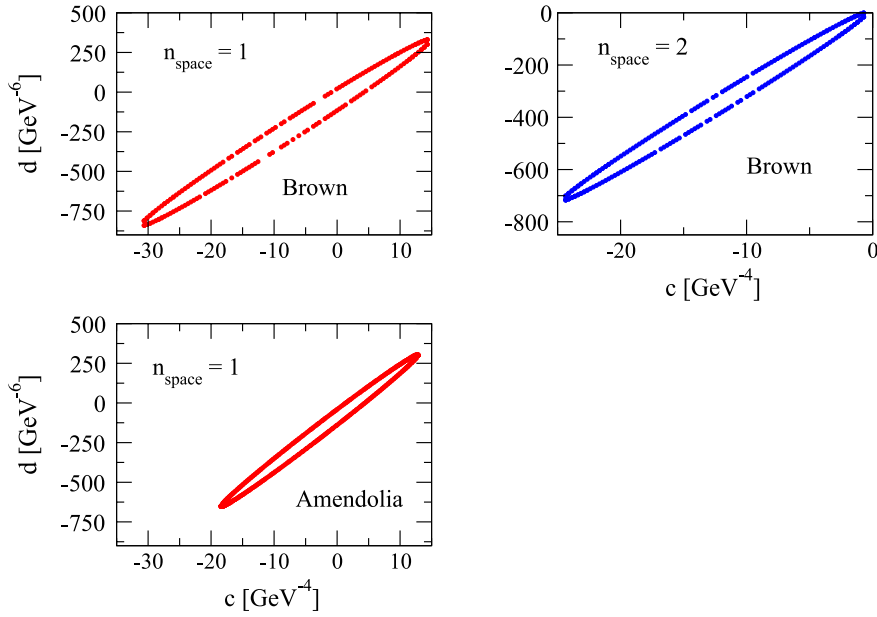
Fig. 5. Constraints on c and d as the number of spacelike constraints are increased. Here the spacelike data are taken from [9, 15]
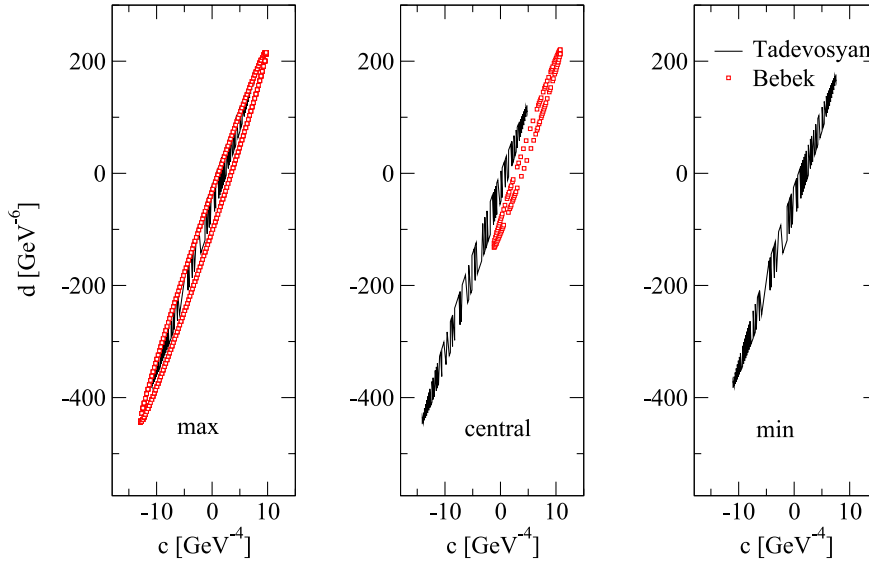

Fig. 6. Variations in the bounds on c and d as data from [10, 16] are varied within their error bounds for three spacelike constraints. The shaded region represents the bounds from [16] and the symbol represents those from [10]

tral values tabulated in Tables 1–4, we see that we are able to use up to three spacelike constraint with the data from Bebek et al. [10] and the recent data from Tadevosyan et al. [16], while we are able to incorporate only two space-like constraints with the data from Brown et al. [9] and one with the data from Amendolia et al. [15]. The best estimate for the bounds on the Taylor coefficient c and d is obtained for the data from Bebek et al. [10]. But varying the Bebek data within the error bounds, we see that there is overlap with the bounds obtained with the data from Tadevosyan et al. [16], as seen in Fig. 6. In Fig. 6, the label "max" refers to the data taken from Tables 1 and 3 with the corresponding error bounds added, i.e. at the upper limit of the error bound, "central" refers to the central values and "min" refers to central value minus the error bound, i.e., the lower limit of the error bound. We see that an overlap between the bounds obtained from the different data set

occurs when the data are close to the upper error bound. In fact at the upper error bound, the data from Tadevosyan et al. give better bounds on the expansion coefficients compared to the data from Bebek et al. At the central value of $F_\pi(t)$, the data from Bebek et al. do better, while at the lower end, the data from Bebek et al., no longer yield stable results, while the data from Tadevosyan et al. still give reasonable bounds. We find that despite small differences in the allowed regions, the fact that the allowed regions are essentially the same offers an important consistency check on the determinations of the form factor by each of the experiments.

As seen from our results so far, the bounds on the Taylor coefficients vary due to the errors in the data presented in Tables 1–4; hence it is important to examine the sensitivity of our results to the inputs. We have made a systematic study of the sensitivity by varying
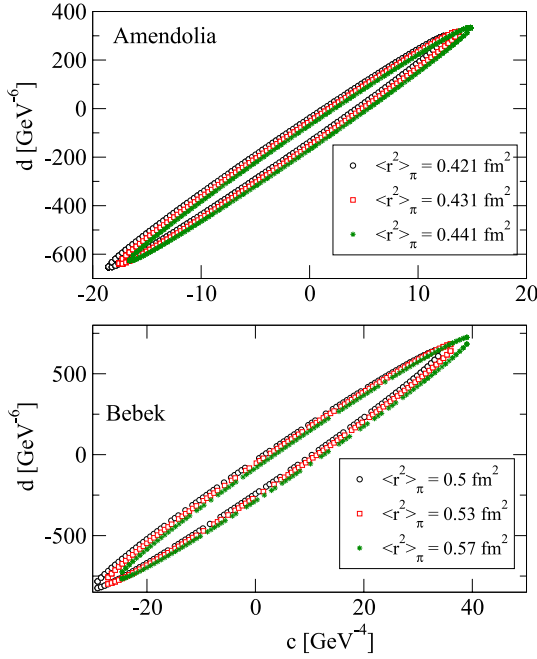
Fig. 7. Variations in the bounds on c and d when the value of r_π is changed. This has been carried out for one spacelike constraint for the data set by Amandolia et al. [15]
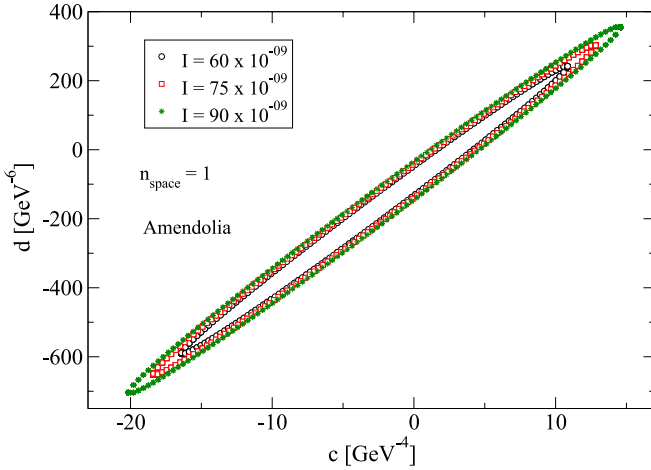

Fig. 8. Variations in the bounds on c and d when the value of I is changed. This has been carried out for one spacelike constraint for the data set by Amandolia et al. [15]

(a) the input value of r_π,
(b) the input value of I, and
(c) varying the experimental determinations of $F_\pi(t)$ within their quoted errors, and in each instance keeping all other inputs fixed.

Variations in the bounds on c and d for one spacelike constraint from [10, 15], when the value of r_π is varied within the error bounds quoted therein, are shown in Fig. 7. We see that the bounds do not vary much as r_π is varied within the allowed errors of a few percent. Figure 8 shows the variations in the bounds of c and d as the value
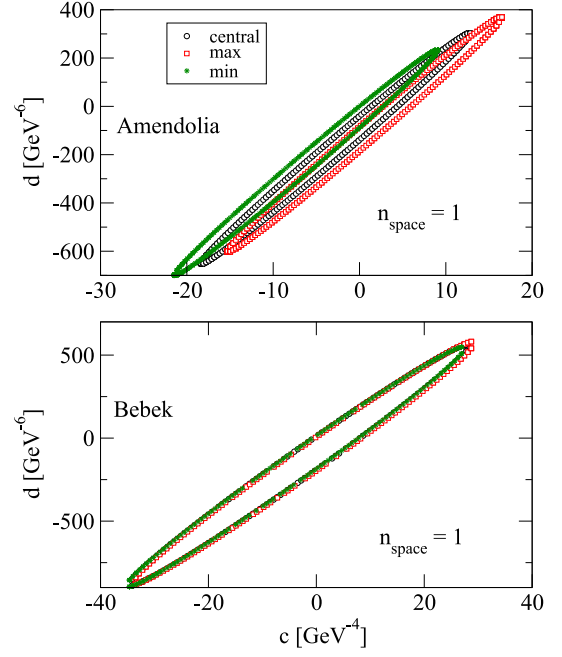

Fig. 9. Variations in the bounds on c and d when the data for $F_\pi(t)$ from Tables 1 and 4 are varied within their error bounds. Here "central" refers to the value without the errors and "min" to the lowest value and "max" to the highest value within the error bounds. Note that the bounds are more sensitive to the errors in the data from the small $|t|$ region
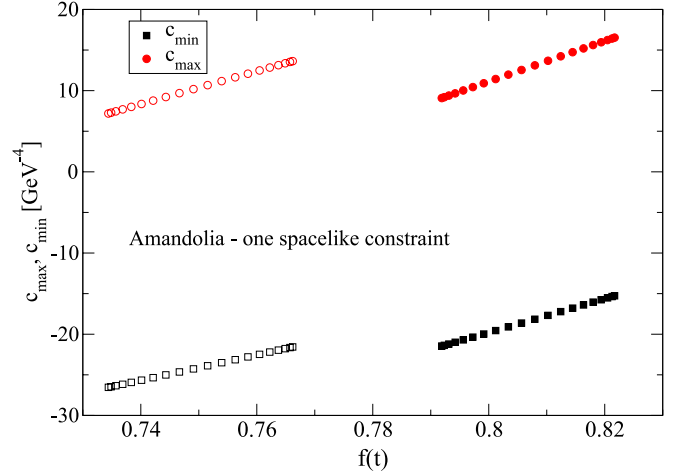

Fig. 10. Variations in the bounds on c when the data for $F_\pi(t)$ from Table 4 are varied within their error bounds. The *filled circles* and *squares* refer to the maximum and minimum of the bounds on c obtained from the first entry in Table 4 and the open ones correspond to the second entry in the table

of I is changed. Lower I values result in a subspace of the region allowed for the coefficients at higher I values. We expect this behavior as our method gives only an allowed region for the coefficients. This explicitly demonstrates that as long as the true pionic contribution is lower than the values we have used, the allowed region lies within the isolated ellipse.
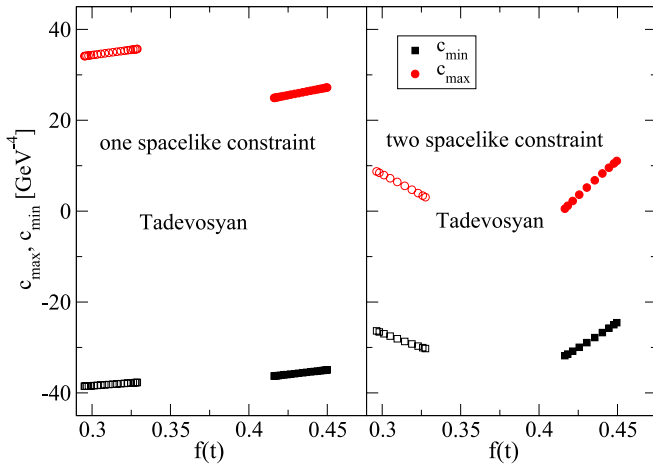
Fig. 11. Variations in the bounds on c when the data for $F_\pi(t)$ from Table 3 are varied within their error bounds. The *filled circles* and *squares* refer to the maximum and minimum of the bounds on c obtained from the first entry in Table 3 and the open ones correspond to the second entry in the table. The *left panel* shows the variation on one spacelike constraint while the *right panel* shows variations on two spacelike constraints. For two spacelike constraints, we fix one constraint at the central value and vary the other over the quoted error bounds [10] and plot the variations in the bounds on c as a function of the constraint that is varied
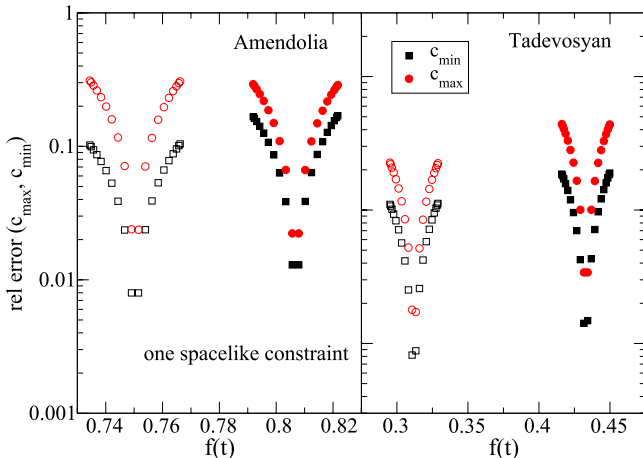

Fig. 12. Relative errors in the bounds on c with respect to the central value, for one spacelike constraint as the constraint is varied over the error bounds for the data sets [15, 16]

Figure 9 shows the variation bounds on c and d for the data from Amendolia et al. [15] and Bebek et al. [10] for one spacelike constraint (smallest magnitude of $|t|$ in Tables 1 and 4). The data are varied within their experimental bounds and the results are depicted in Fig. 9. We see that the bounds on the expansion coefficients are most sensitive to errors in the data from lower $|t|$. Having said all that, it is our view that one may read off reliable ranges for both c and d in light of this sensitivity analysis. However, an analogous sensitivity test that we have carried out for two spacelike constraints for the data from Amendolia et

al. [15] leads to a complete loss of coherence. This is an unavoidable numerical difficulty in the determinant that arises due to the fact that the entries are small and closely spaced. Therefore we can conclude that for low $|t|$ information we are unable to obtain reliable results for more than one constraint.

We explore this sensitivity of the bounds to the data taken from the low $|t|$ region using one spacelike constraint from [15] and varying this constraint over the given error bounds (Table 4) and study the corresponding variations in the bounds on c alone. This is seen in Fig. 10, where the circles represent the maximum and the squares represent the minimum of the bounds. The filled symbols stand for the bounds obtained from the data at lower value of $|t|$ and the open symbols represent those from the data at higher value of $|t|$. Figure 11 shows similar variations in the bounds on c when one as well as two spacelike constraints (Table 3) for the data taken from [16] are varied over the error bounds. Note that the data from [16] lie at a higher $|t|$ value compared to the data from [15]. When two spacelike constraints are used, we fix one constraint at the central value and vary the other over the error bounds quoted in [16] and plot the maximum and minimum of the bounds as a function of the constraint that is varied. From Figs. 10 and 11, we see that data from a lower $|t|$ value in each set constrain the coefficients better for one spacelike constraint. Also the sensitivity to the error bounds is greater for a set at lower $|t|$ compared to the set at higher value of $|t|$. We also note that two spacelike constraints are more sensitive to the variations in $F_\pi(t)$ compared to one spacelike constraint, as can be seen in Fig. 11.

Relative errors in the bounds on c as one spacelike constraint is varied over the quoted error bounds compared to the bounds obtained from the central value are shown in Fig. 12 for the data sets from Amendolia et al. and Tadevosyan et al. We see that the relative errors are smaller for the data from Tadevosyan et al., once again emphasizing our earlier observation that the sensitivity of the Taylor coefficients to the errors in the determination of $F_\pi(t)$ is greater for the data from the low $|t|$ region compared to those from the high $|t|$ region.

4 Discussion and conclusions

In this work we have considered the constraints on the pion electromagnetic form factor coming from present day estimates of the pionic contributions to the muon anomaly, and from spacelike data that are available over a fairly extended kinematic regime. We have adopted the framework of Raina and Singh and have extended it to obtain constraints on c and d, the expansion coefficients sub-leading to the charge radius of the pion. We have used data available since the 1970's (also used in [11]) and more recent data, which span significantly lower values of $|t|$, as well as very recent data coming from Tadevosyan et al., which are at higher $|t|$ values, which lie in the range of Bebek et al.

As mentioned in the introduction, Caprini [5] has used timelike data to obtain constraints on the Taylor coeffi-

cients. By systematically considering the inclusion of only the phase, the ellipse with no constraints was found to shrink considerably, using as an observable the QCD polarization function (see Figs. 1 and 2 in [5]). This analysis employs an optimal technique, resulting in an integral equation of the Fredholm type that was solved numerically. The ellipse was found to shrink even further when both the phase as well as the modulus information were used even though the technique was non-optimal (see Fig. 3 in [5]). Questions remain about its validity due to certain mathematical difficulties, as discussed by Caprini.

The best estimates for the bounds on c and d are obtained using the data from Bebek et al. [10] for three spacelike constraints. In Fig. 13, we compare our best result with those obtained by Caprini using only the phase from the timelike region. Using spacelike data we get the following range for the expansion coefficients: $-1\,\mathrm{GeV}^{-4} \lesssim c \lesssim 11\,\mathrm{GeV}^{-4}$ and $-132\,\mathrm{GeV}^{-6} \lesssim d \lesssim 220\,\mathrm{GeV}^{-6}$. On the other hand Caprini has a range of $[-14\,\mathrm{GeV}^{-4},\ 44\,\mathrm{GeV}^{-4}]$ and $[-236\,\mathrm{GeV}^{-6},\ 594\,\mathrm{GeV}^{-6}]$ for c and d respectively using only the phase of the timelike data. It is interesting to note that the overlap region between the two determinations, ours using spacelike data and the muon anomaly and Caprini's using the phase of timelike data and the QCD polarization observable, accommodates comfortably the value of c from chiral perturbation theory. We note here that similar bounds obtained using the central values of the Tadevosyan data (Table 3) using three spacelike constraints do not accommodate the value of c obtained from chiral perturbation theory, but varying the data at the upper end of the error bound, as in Fig. 6, the allowed region does include this value.

Our conclusions are that the constraints are weaker than those obtained by Caprini using both phase and modulus of the data from the timelike region (see Fig. 3 in [5]), while they are more stringent than those obtained with only the phase of the timelike data. Here we note again that the latter of these treatments is rigorous and the results may be taken as reliable. On the other hand, the results obtained using both the modulus and phase while appearing more stringent are on a less rigorous footing, due to inherent mathematical difficulties as noted in [5].

We have also carried out a sensitivity analysis by varying the estimate for the pionic contribution over a significant range, varying the charge radius over its presently known errors, and also by varying the experimental data that we use over its errors, for the values of $|t|$ that we have chosen. Our conclusions are that in the small $|t|$ region, the system is very sensitive and as a result, we have been unable to implement anything more than one spacelike constraint. For larger values, we are able to include two and even three constraints.

Of related interest is the extreme sensitivity of the system when bounds are being derived on the muon anomaly from the spacelike data, as recognized earlier by Pantea and Raszillier [17]. The issue was of some significance because several spacelike constraints were being used to obtain these bounds. Our circumstances are somewhat mitigated by the fact that we are using a significantly smaller number of constraints, as the determinantal equations we are solving are already of rather large dimensions. By studying the sensitivity of the bounds, we are confident that our results remain stable.

It is conceivable that as the data improve one may obtain better constraints on c and d, where it is numerically feasible; that can then be used as input for high precision, self-consistent determinations of the form factor. We also note at this point that our work takes into account only the information present in the spacelike region. It would be worthwhile to properly formulate the problem so that the information available in the timelike region could be incorporated together with a comprehensive error analysis. A theory of error functionals has been developed by Raina and Singh [18] in the context of finding a lower bound for the muon anomaly, which could in principle be extended for the problem at hand, which is beyond the scope of this work. Therefore, future investigations could combine highly accurate phase and modulus timelike information coming from recent experiments and the techniques developed by Caprini for the phase problem, together with a suitable extension of the error functional method, to produce stringent constraints on c and d

Fig. 13. Comparing our best ellipse obtained for three spacelike constraints using data from Bebek et al. [10] (*symbol*) with the result obtained using the phase of the form factor in the timelike region (see Fig. 2 in [5])

References

1. V. Singh, A.K. Raina, Fortschr. Phys. **27**, 561 (1979)
2. J.P. Miller, E. de Rafael, B.L. Roberts, Rep. Prog. Phys. **70**, 795 (2007) [arXiv:hep-ph/0703049]
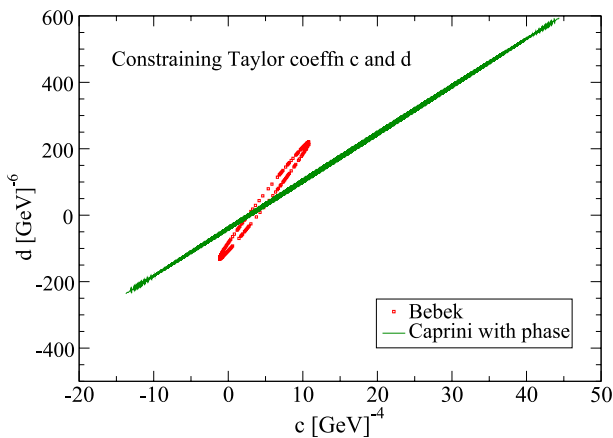3. F. Jegerlehner, Acta Phys. Pol. B **38**, 3021 (2007) [hep-ph/0703125]

4. D. Palmer, Phys. Rev. D **4**, 1558 (1971)
5. I. Caprini, Eur. Phys. J. C **13**, 471 (2000) [hep-ph/9907227]
6. C. Bourrely, I. Caprini, Nucl. Phys. B **722**, 149 (2005) [hep-ph/0504016]
7. J. Bijnens, P. Talavera, JHEP **0203**, 046 (2002) [hep-ph/0203049]
8. C.J. Bebek et al., Phys. Rev. D **9**, 1229 (1974)
9. C.N. Brown et al., Phys. Rev. D **8**, 92 (1973)
10. C.J. Bebek et al., Phys. Rev. D **13**, 25 (1976)
11. A.K. Raina, V. Singh, J. Phys. G **3**, 315 (1977)
12. G. Nenciu, I. Raszillier, Nuovo Cim. A **11**, 319 (1972)
13. E.B. Dally et al., Phys. Rev. Lett. **39**, 1176 (1977)
    E.B. Dally et al., Phys. Rev. D **24**, 1718 (1981)
14. E.B. Dally et al., Phys. Rev. Lett. **48**, 375 (1982)
15. NA7 Collaboration, S.R. Amendolia et al., Nucl. Phys. B **277**, 168 (1986)
16. Jefferson Lab F(pi) Collaboration, V. Tadevosyan et al., Phys. Rev. C **75**, 055 205 (2007) [nucl-ex/0607007]
17. D. Pantea, I. Raszillier, FT-132-1977 (preprint)
18. A.K. Raina, V. Singh, Nucl. Phys. B **139**, 341 (1978)